Runaway of energetic test ions in a toroidal plasma

S. Eilerman, J. K. Anderson, J. S. Sarff, C. B. Forest, J. A. Reusch, M. D. Nornberg, and J. Kim

Citation: Physics of Plasmas (1994-present) **22**, 020702 (2015); doi: 10.1063/1.4907662
View online: http://dx.doi.org/10.1063/1.4907662
View Table of Contents: http://scitation.aip.org/content/aip/journal/pop/22/2?ver=pdfcov
Published by the AIP Publishing

Runaway of energetic test ions in a toroidal plasma

S. Eilerman,[a] J. K. Anderson, J. S. Sarff, C. B. Forest, J. A. Reusch, M. D. Nornberg, and J. Kim
Department of Physics, University of Wisconsin–Madison and Center for Magnetic Self-Organization in Laboratory and Astrophysical Plasmas, Madison, Wisconsin 53706, USA

(Received 22 December 2014; accepted 21 January 2015; published online 3 February 2015)

Ion runaway in the presence of a large-scale, reconnection-driven electric field has been conclusively measured in the Madison Symmetric Torus reversed-field pinch (RFP). Measurements of the acceleration of a beam of fast ions agree well with test particle and Fokker-Planck modeling of the runaway process. However, the runaway mechanism does not explain all measured ion heating in the RFP, particularly previous measurements of strong perpendicular heating. It is likely that multiple energization mechanisms occur simultaneously and with differing significance for magnetically coupled thermal ions and magnetically decoupled tail and beam ions. © *2015 AIP Publishing LLC*. [http://dx.doi.org/10.1063/1.4907662]

Unlike many other physical systems, plasmas exhibit an interesting phenomenon in which the collision frequency of a test particle decreases as the particle's speed increases. As a result, an external force (such as an applied electric field) that overcomes a particle's frictional drag can increasingly accelerate the particle to very high energies. The conditions for electron runaway were calculated by Dreicer in 1958,[1] and electron runaway has frequently been observed in laboratory experiments.[2] A theory for ion runaway in fusion-relevant plasmas was developed later,[3] and while ion runaway is believed to be an important process in solar flares[4] and lightning discharges,[5] runaway ions have only recently been observed in laboratory plasmas.[6,7] In one example, a strong electric field induced by equilibrium changes during reconnection events in the Mega Ampere Spherical Tokamak (MAST) causes measurable parallel ion heating, and good agreement between a Monte Carlo orbit calculation and neutral particle analyzer (NPA) measurements of the energetic ion tail identify ion runaway as the dominant acceleration mechanism.[6] However, the clear runaway of test ions has not been directly measured in laboratory or astrophysical plasmas.

The anomalous heating and acceleration of ions has been the focus of many studies on various reversed-field pinch (RFP) devices[8–17] and is also of great interest in astrophysical plasmas.[18–21] In the Madison Symmetric Torus (MST),[22] energy stored in the equilibrium magnetic field can transiently drop at rates exceeding 200 MW during reconnection events, and roughly 10%–25% of that energy is converted into ion energy.[14] Several features of the heating process and resulting ion distribution have been identified, including the dependence of heating efficiency on ion mass,[14] the generation of a non-Maxwellian energetic ion tail,[15] $T_\perp > T_\parallel$ anisotropy of the C^{+6} impurity distribution,[15] and a Z/μ dependence in heating rate for impurities.[16] However, no single energization mechanism has been able to explain all of the observed phenomena.

Ion runaway in the reversed-field pinch is associated with periodic, impulsive reconnection events that cause self-organization of the magnetic equilibrium and the spontaneous generation of a large, axisymmetric inductive electric field. These events are also accompanied by strong magnetic fluctuations from unstable, current-driven tearing modes which cause enhanced energy and particle transport.[23–26] Fast ions, however, are relatively insensitive to the tearing-mode-driven fluctuations and have near-classical confinement.[27,28] Despite their comparatively good confinement, fast ions may still experience pitch-angle scattering from the magnetic fluctuations,[29] a process important in cosmic ray shock acceleration.[30] Such scattering could inhibit the runaway process.

In this letter, we experimentally test the ion runaway mechanism on the MST reversed-field pinch. A time series of equilibrium reconstructions[31,32] throughout the reconnection event are used to measure the large-scale, axisymmetric component of the electric field profile. The equilibrium reconstructions employ a three-parameter fit to the current profile and are constrained by a number of MST's diagnostics. These reconstructions include Faraday rotation measurements using a far-infrared laser polarimeter, which alone provides an accurate measurement of the local electric field in the core region where the fast ions are located.[33] The parallel component of the computed field is core-peaked and reaches amplitudes of 40–100 V/m (depending on plasma conditions) for roughly 200 μs (Fig. 1(a)). While the previously mentioned experiments have largely focused on thermal ion heating, a recently installed tangential neutral beam injector allows the reconnection process to be probed with a well-known population of energetic test ions.[34,35] The beam can inject a neutral flux equivalent to 40 A of ion current at energies ranging from 10 to 25 keV (much greater than the typical ion temperature of 500–1000 eV). The beam is capable of injecting either hydrogen or deuterium; all experiments presented in this work use hydrogen as the primary injected species. The fast ion population is studied using a compact $\mathbf{E} \parallel \mathbf{B}$ neutral particle analyzer.[36,37] The NPA views the plasma tangentially, and modeling suggests the measured signal is predominately influenced by high-pitch ($v_\parallel/|v| \sim 1$), core-localized beam ions despite the lack of an active neutral particle source.[38,39]

NPA data throughout a reconnection event are shown in Fig. 2. Many similar events are averaged together to reduce

[a]eilerman@wisc.edu

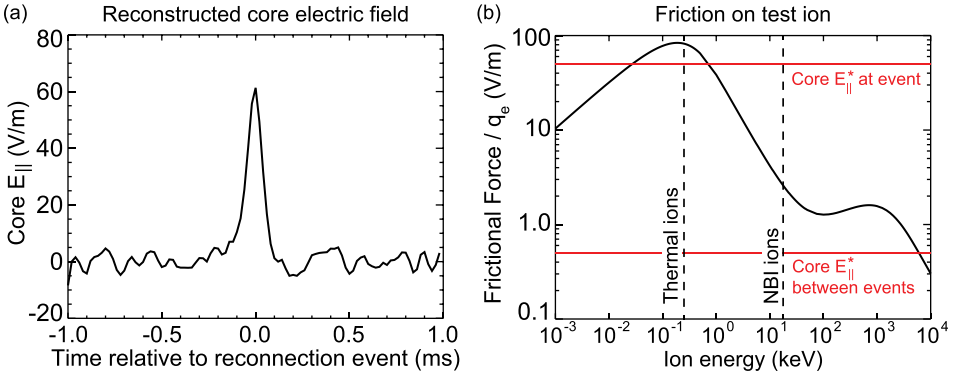

FIG. 1. (a) The parallel electric field induced by the change in equilibrium magnetic fields typically peaks between 40–100 V/m in the core. (b) The frictional force on a test ion (black) has two local maxima corresponding to electron and ion drag, respectively. The effective parallel electric field (red) is capable of driving runaway for beam-injected ions during the ~200 μs duration of the reconnection event.

statistical noise. Prior to the event at $t = 0$, a beam distribution is observed at the injection energy of 19 kV. This distribution is representative of the fast ion behavior in the absence of reconnection events. At the event, the beam ions clearly accelerate to higher energies. Neutral beam injection is turned off at the time of the reconnection event so that the accelerated distribution can be studied without additional sourcing of ions at the injection energy. The amount of energy gained by the test ions at the event is quantified by taking the average of the distribution function $\langle U \rangle = \int f(U)\, dU$, where $f(U)$ is calculated from the calibrated NPA data.[37,39] Note that the acceleration of the energetic ions occurs continuously during the ~0.2 ms duration of the transient electric field pulse shown in Fig. 1(a), during which the ions complete approximately 40 toroidal transits. The average energy remains relatively constant after the event due to the good confinement of energetic ions ($\tau_{fi} \geq 20$ ms), discussed later in this paper.

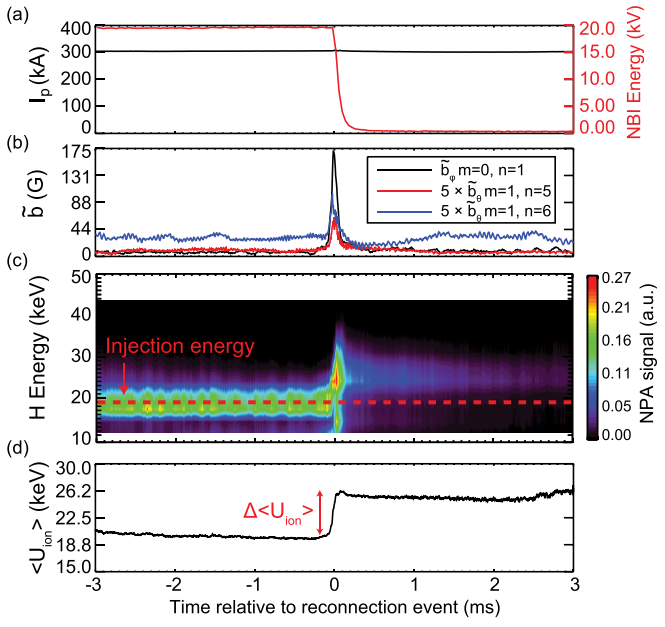

FIG. 2. (a) The plasma current is relatively constant throughout the reconnection event, and the NBI is switched off at the event so that the accelerated ion distribution can be studied. (b) Magnetic fluctuations associated with tearing modes are used as a time marker for averaging many similar reconnection events and reducing statistical noise. (c) An NPA spectrogram illustrates the acceleration of the beam population at the reconnection event. Towards the bottom of the panel, the acceleration of the beam's half-energy component is seen at $t = 0$. (d) The average energy of the underlying fast ion distribution is calculated from the NPA data.

To determine whether the observed acceleration is caused by ion runaway, a test particle model using the Furth-Rutherford formalism is employed.[3] The effect of the inductive electric field on a test particle is calculated by solving the differential equation

$$\frac{dv_\parallel}{dt} = \frac{q}{m}\int \left(E_\parallel^*(\mathbf{r},t) - \mathcal{F}(\mathbf{r},t)\right)dt, \tag{1}$$

where $E_\parallel^*$ is the parallel component of the effective electric field[3,6] and $\mathcal{F} = mv_\parallel(\nu_s^{b/e} + \nu_s^{b/i})$ is the classical friction that beam test ions experience from background electron and ion collisions. For typical MST parameters, $E_\parallel^* \simeq 0.85E_\parallel$, which is greater than the friction for fast, beam-injected ions and is on the order of the friction felt by thermal ions (Fig. 1(b)). The test particle is assumed to spatially average over the magnitude of the parallel electric field within one gyroradius (≃4 cm) of the core.

The predictions of this simple model agree well with the NPA measurements (Fig. 3). A number of experiments confirm that the parallel inductive electric field is the dominant mechanism accelerating these ions. The beam injection energy was varied, and the amount of energy gain scales with the initial ion energy as predicted by the runaway model. A number of plasma parameters (current, density, $q(a)$) were altered, and in each case the changes in the electric field calculated from equilibrium reconstructions agreed with the measured change in ion energy gain (in Fig. 3, data from two different densities are shown). Individual events within a single dataset also show a strong correlation between the strength of the reconnection event (approximated by measurements of the loop voltage) and the NPA-measured change in the energetic ion distribution.

Reversing the plasma current flips the direction of the induced electric field while the velocity of the fast beam ions remains the same. In these "counter-injection" cases, the ions are observed to decelerate rather than accelerate, in agreement with the electric field magnitude and direction. This directional dependence is the most conclusive evidence that the large-scale, axisymmetric parallel electric field is responsible for the observed acceleration. Further experiments were performed with the NPA on a radial viewport so that the measurement samples only the perpendicular component

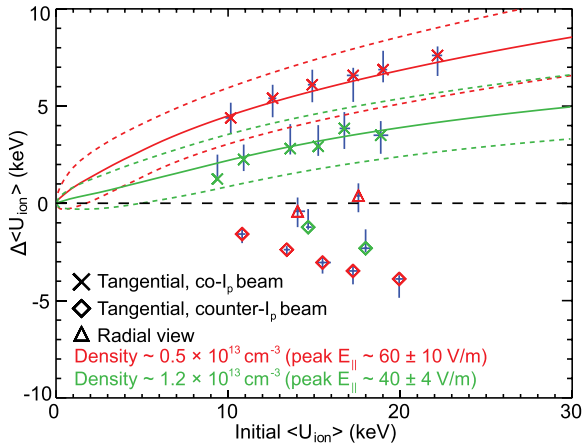

FIG. 3. Each data point represents an ensemble of NPA measurements from a given injection energy in one of two plasma conditions and three viewing geometries. For co-current beam injection (crosses), ion energy gain increases with initial ion energy. The acceleration is stronger in lower density plasmas with higher core electric fields (color-coded). Deceleration is observed in counter-I_p beam injection (diamonds). Data from a radial viewport (triangles) indicate no perpendicular acceleration. Solid lines represent the best fit to data using a test particle model with reasonable assumptions about Z_{eff} and the position of the detected ions. Dotted lines depict Monte Carlo variation within the uncertainty of the model parameters (including the modeled spatial and pitch profiles of the NPA measurement).

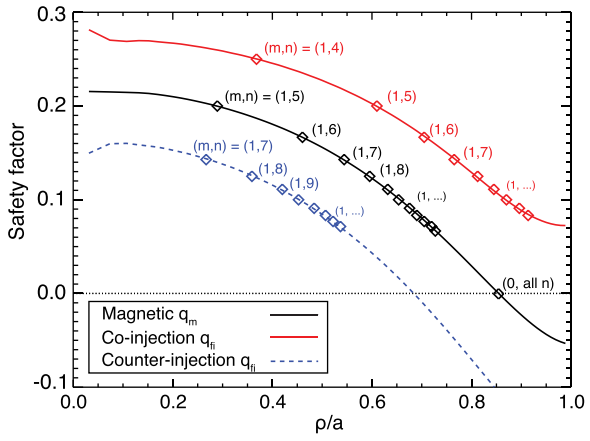

FIG. 4. The magnetic safety factor q_m (black) is plotted along with the effective safety factor of the fast ions q_{fi} for co-current (red solid) and counter-current (blue dotted) beam injection at 25 keV and pitch $v_\parallel/|v| = 0.85$. The location of resonant surfaces for several $m = 1$ tearing modes is plotted overtop q_m, and the analogous resonances in the fast ion trajectories are similarly labeled. The motion of co-injected fast ions in the core ($n \leq 4$) is not resonant with any tearing modes in the plasma; however, the high-n tearing modes at larger radii will affect the counter-injected fast ions in the core due to the global nature of their eigenfunctions.

of ion velocity space. In these experiments, no perpendicular acceleration is measurable within diagnostic uncertainty.

Whereas electron runaway was observed during reconnection events in MAST,[6] previous x-ray spectrum measurements and Fokker-Planck modeling have shown that few energetic electrons appear for the MST plasma conditions discussed here.[26] The lack of runaway electrons is a result of the large stochastic magnetic transport associated with multiple tearing modes spread across the plasma's minor radius. The strong sensitivity of electrons to stochastic transport is best revealed in different plasma conditions in which the tearing mode amplitudes and stochastic transport are reduced using current profile control. The modeling of electrons in this improved-confinement case[26] is consistent with the formation of an energetic electron tail.

The agreement between the observed fast ion acceleration and the ion runaway model is therefore very significant. This implies that the particle acceleration is provided by the axisymmetric component of the electric field, and that the fast ion interaction with magnetic fluctuations is weak. It has been shown previously that, in the RFP, fast ions are relatively insensitive to tearing-mode-driven magnetic fluctuations and have near-classical confinement, much larger than the thermal particle confinement time ($\tau_{fi} \sim 25\ \tau_p$).[28] The displacement of the fast ion guiding center from magnetic field lines[27] allows these particles to decouple from the tearing-mode-driven fluctuations and their resulting electromotive forces. Core localized, co-injected ions have an effective safety factor $q_{fi} = \frac{rv_\phi}{Rv_\theta}$ greater than the magnetic safety factor q_m; with the RFP's monotonically decreasing safety factor profile, the resonant motion of the ion guiding center can have a toroidal mode number larger than any tearing instabilities within the plasma (Fig. 4). The deviation $\Delta q = q_{fi} - q_m$ approaches zero as ion energy is decreased to thermal levels and particle motion becomes dominated by the tearing mode fluctuations.

For counter-injected fast ions, $q_{fi} < q_m$, allowing the ions to interact with the resonant tearing modes at larger radii. This interaction is evident in the dramatic difference between the near-classical confinement of co-injected ions and the relatively poor confinement of counter-injected ions ($\tau_{fi}^{counter} \sim 2.5\ \tau_p$).[28] In this study, less energy change is observed for counter-injected ions than co-injected ions at a given initial energy: considering a reflection of the solid lines in Fig. 3, the model clearly over-predicts the measured energy change in the counter-injection experiments, suggesting that tearing mode fluctuations impact the counter-injected ions and their behavior cannot be determined from only the axisymmetric component of the electric field.

Because of the insensitivity of the co-injected fast ions to magnetic fluctuations, a time-dependent analysis of the ion distribution function can be performed with the CQL3D Fokker-Planck solver[40] using the axisymmetric component of electric field as the driving term. Initial distributions of the bulk ions, electrons, and impurities were input according to measurements and equilibrium reconstructions. The initial fast ion distribution is estimated by assuming classical slowing of the injected beam deposition profile calculated from TRANSP/NUBEAM modeling.[35,41] All distributions were evolved through a time-varying electric field matching the reconstructed experimental field. Strong quantitative agreement is observed between the NPA experimental measurement and the acceleration of modeled fast ions detected by a synthetic NPA diagnostic (Fig. 5(a)). The CQL3D modeling of bulk and impurity ions shows predominately parallel energization and a slow rise in the perpendicular energy; these features are not consistent with previous measurements which indicate a quick rise in perpendicular temperature and $T_\perp > T_\parallel$ anisotropy for the C^{+6} impurities.[14,15] Fluctuation-

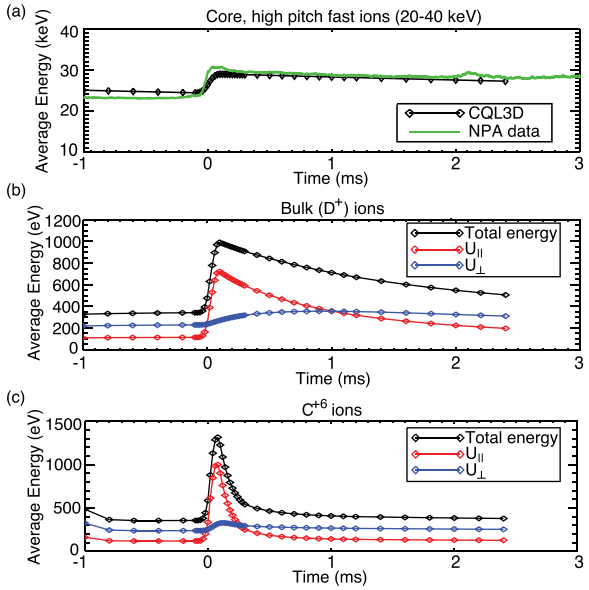

FIG. 5. CQL3D is used to model changes to the beam ions (a), bulk ions (b), and C^{+6} impurity ions (c) due to an electric field pulse at $t = 0$ matching the electric field from equilibrium reconstructions. The portion of the CQL3D distribution corresponding to fast beam ions within the NPA detection range accelerates in a manner consistent with experimental data (a). For the thermal and impurity ions, CQL3D predicts an energy anisotropy with $U_{\|} > U_{\perp}$ and a slow rise in the perpendicular energy, which is inconsistent with previous experimental results.

driven electromotive forces are critical to the dynamics of thermal particles in the reversed-field pinch,[13] and the large magnetic fluctuations present during a reconnection event are not incorporated in the CQL3D model, making it inappropriate for study of the thermal ion behavior. However, the fast beam-injected ions are sufficiently decoupled from the magnetic fluctuations that CQL3D is able to reproduce their behavior. Ongoing work using the RIO particle tracing code[27,42] (which does include magnetic fluctuations) will further explore the effect of the parallel electric field on thermal particles; however, it is hard to imagine a scenario where such a field will reproduce features such as the C^{+6} $T_{\perp} > T_{\|}$ anisotropy observed in the experiment. Rather, it is posited that multiple energization mechanisms must be occurring simultaneously, affecting thermal and suprathermal particles differently according to their degree of magnetic coupling and consequentially their susceptibility to fluctuation-based electromotive forces.

In conclusion, the runaway of test ions has been experimentally measured in a toroidal plasma. Fast ions sourced with a neutral beam injector are used to directly probe the runaway process for the first time, whereas previous results in toroidal confinement devices have relied on measurements of bulk ion heating. The fast test ions meet the runaway criteria put forth by Furth and Rutherford and accelerate up to 110%–130% of their initial energy during short-duration, high-magnitude parallel electric fields induced by magnetic equilibrium changes during periodic magnetic reconnection events. These measurements agree with the acceleration expected from a simple test particle model as well as the CQL3D Fokker-Planck model. The magnitude of acceleration depends on initial ion energy and plasma conditions, particles decelerate when the direction of the electric field is reversed, and no energy change is observed perpendicular to the background magnetic field. Due to the parallel nature of the runaway mechanism, it is unlikely that it is solely responsible for the long-studied anomalous heating of thermal ions during reconnection in the RFP which is thought to be a predominately perpendicular process. However, the runaway mechanism may be important for ions in the previously identified suprathermal tail,[15] and future studies of anomalous ion heating and acceleration in the RFP will need to consider the role of ion runaway alongside any other proposed mechanisms.

The authors wish to acknowledge R. W. Harvey at CompX for his work on the CQL3D time-varying electric field module in support of this manuscript. This material is based upon work supported by the U.S. Department of Energy Office of Science, Office of Fusion Energy Sciences program under Award No. DE-FC02-05ER54814 and the National Science Foundation under Grant No. PHY 08-21899.

[1]H. Dreicer, Phys. Rev. **115**, 238 (1959).
[2]H. Knoepfel and D. A. Spong, Nucl. Fusion **19**, 785 (1979).
[3]H. P. Furth and P. H. Rutherford, Phys. Rev. Lett. **28**, 545 (1972).
[4]G. D. Holman, Astrophys. J. **452**, 451 (1995).
[5]T. Fülöp and M. Landreman, Phys. Rev. Lett. **111**, 015006 (2013).
[6]P. Helander, L. G. Eriksson, R. J. Akers, C. Byrom, C. G. Gimblett, and M. R. Tournianski, Phys. Rev. Lett. **89**, 235002 (2002).
[7]S. Raychaudhuri, S. K. Saha, S. Chowdhury, D. Banik, and A. K. Hui, Phys. Plasmas **13**, 122510 (2006).
[8]R. B. Howell and H. J. Karr, Phys. Fluids **19**, 2012 (1976).
[9]R. B. Howell and Y. Nagayama, Phys. Fluids **28**, 743 (1985).
[10]G. A. Wurden, P. G. Weber, K. F. Schoenberg, A. E. Schofield, J. A. Phillips, C. P. Munson, G. Miller, J. C. Ingraham, R. B. Howell, J. N. Downing, R. E. Chrien, T. E. Cayton, L. C. Burkhardt, R. J. Bastasz, S. E. Walker, A. M. Preszler, P. G. Carolan, and C. A. Bunting, in Proceedings of the 15th European Conference on Controlled Fusion and Plasma Physics, Dubrovnik, Yugoslavia, 16 May 1988, Los Alamos National Laboratory Technical Report No. LA-UR-88-895.
[11]T. Fujita, K. Saito, J. Matsui, Y. Kamada, H. Morimoto, Z. Yoshida, and N. Inoue, Nucl. Fusion **31**, 3 (1991).
[12]E. Scime, S. Hokin, N. Mattor, and C. Watts, Phys. Rev. Lett. **68**, 2165 (1992).
[13]S. Gangadhara, D. Craig, D. A. Ennis, D. J. Den Hartog, G. Fiksel, and S. C. Prager, Phys. Plasmas **15**, 056121 (2008).
[14]G. Fiksel, A. F. Almagri, B. E. Chapman, V. V. Mirnov, Y. Ren, J. S. Sarff, and P. W. Terry, Phys. Rev. Lett. **103**, 145002 (2009).
[15]R. M. Magee, D. J. Den Hartog, S. T. A. Kumar, A. F. Almagri, B. E. Chapman, G. Fiksel, V. V. Mirnov, E. D. Mezonlin, and J. B. Titus, Phys. Rev. Lett. **107**, 065005 (2011).
[16]S. T. A. Kumar, A. F. Almagri, D. Craig, D. J. Den Hartog, M. D. Nornberg, J. S. Sarff, and P. W. Terry, Phys. Plasmas **20**, 056501 (2013).
[17]M. S. Cartolano, D. Craig, D. J. Den Hartog, S. T. A. Kumar, and M. D. Nornberg, Phys. Plasmas **21**, 012510 (2014).
[18]E. R. Priest, C. R. Foley, J. Heyvaerts, T. D. Arber, J. L. Culhane, and L. W. Acton, Nature **393**, 545 (1998).
[19]S. R. Cranmer, J. L. Kohl, G. Noci, E. Antonucci, G. Tondello, M. C. E. Huber, L. Strachan, A. V. Panasyuk, L. D. Gardner, M. Romoli, S. Fineschi, D. Dobrzycka, J. C. Raymond, P. Nicolosi, O. H. W. Siegmund, D. Spadaro, C. Benna, A. Ciaravella, S. Giordano, S. R. Habbal, M. Karovska, X. Li, R. Martin, J. G. Michels, A. Modigliani, G. Naletto, R. H. O'Neal, C. Pernechele, G. Poletto, P. L. Smith, and R. M. Suleiman, Astrophys. J. **511**, 481 (1999).
[20]J. Heyvaerts and E. R. Priest, Astron. Astrophys. **137**, 63 (1984).
[21]E. G. Zweibel and M. Yamada, Annu. Rev. Astron. Astrophys. **47**, 291 (2009).

[22]R. N. Dexter, D. W. Kerst, T. W. Lovell, S. C. Prager, and J. C. Sprott, Fusion Technol. **19**, 134 (1991).
[23]G. Fiksel, S. C. Prager, W. Shen, and M. R. Stoneking, Phys. Rev. Lett. **72**, 1028 (1994).
[24]T. M. Biewer, C. B. Forest, J. K. Anderson, G. Fiksel, B. Hudson, S. C. Prager, J. S. Sarff, J. C. Wright, D. L. Brower, W. X. Ding, and S. D. Terry, Phys. Rev. Lett. **91**, 045004 (2003).
[25]M. R. Stoneking, S. A. Hokin, S. C. Prager, G. Fiksel, H. Ji, and D. J. Den Hartog, Phys. Rev. Lett. **73**, 549 (1994).
[26]R. O'Connell, D. J. Den Hartog, C. B. Forest, J. K. Anderson, T. M. Biewer, B. E. Chapman, D. Craig, G. Fiksel, S. C. Prager, J. S. Sarff, S. D. Terry, and R. W. Harvey, Phys. Rev. Lett. **91**, 045002 (2003).
[27]G. Fiksel, B. Hudson, D. J. Den Hartog, R. M. Magee, R. O'Connell, S. C. Prager, A. D. Beklemishev, V. I. Davydenko, A. A. Ivanov, and Y. A. Tsidulko, Phys. Rev. Lett. **95**, 125001 (2005).
[28]J. K. Anderson, W. Capecchi, S. Eilerman, J. J. Koliner, L. Lin, M. D. Nornberg, J. A. Reusch, and J. S. Sarff, Plasma Phys. Controlled Fusion **56**, 094006 (2014).
[29]C. F. Kennel and F. Engelmann, Phys. Fluids **9**, 2377 (1966).
[30]E. G. Zweibel, Phys. Plasmas **20**, 055501 (2013).
[31]J. K. Anderson, C. B. Forest, T. M. Biewer, J. S. Sarff, and J. C. Wright, Nucl. Fusion **44**, 162 (2004).
[32]J. K. Anderson, T. M. Biewer, C. B. Forest, R. O'Connell, S. C. Prager, and J. S. Sarff, Phys. Plasmas **11**, L9 (2004).
[33]W. X. Ding, D. L. Brower, B. H. Deng, A. F. Almagri, D. Craig, G. Fiksel, V. Mirnov, S. C. Prager, J. S. Sarff, and V. Svidzinski, Phys. Plasmas **13**, 112306 (2006).
[34]J. K. Anderson, A. F. Almagri, D. J. Den Hartog, S. Eilerman, C. B. Forest, J. J. Koliner, V. V. Mirnov, L. A. Morton, M. D. Nornberg, E. Parke, J. A. Reusch, J. S. Sarff, J. Waksman, V. Belykh, V. I. Davydenko, A. A. Ivanov, S. V. Polosatkin, Y. A. Tsidulko, L. Lin, D. Liu, G. Fiksel, H. Sakakita, D. A. Spong, and J. B. Titus, Phys. Plasmas **20**, 056102 (2013).
[35]D. Liu, A. F. Almagri, J. K. Anderson, V. Belykh, B. E. Chapman, V. I. Davydenko, P. Deichuli, D. J. Den Hartog, S. Eilerman, G. Fiksel, C. B. Forest, A. A. Ivanov, M. D. Nornberg, S. V. Polosatkin, J. S. Sarff, N. Stupishin, and J. Waksman, in *38th EPS Conference on Plasma Physics* (Strasbourg, France, 2011), Vol. 35G, p. P2.101.
[36]S. V. Polosatkin, V. Belykh, V. I. Davydenko, G. Fiksel, A. A. Ivanov, V. Kapitonov, A. Khilchenko, V. Khilchenko, V. Mishagin, and M. Tiunov, Fusion Sci. Technol. **59**, 259 (2011).
[37]J. A. Reusch, J. K. Anderson, V. Belykh, S. Eilerman, D. Liu, G. Fiksel, and S. V. Polosatkin, Rev. Sci. Instrum. **83**, 10D704 (2012).
[38]S. Eilerman, J. K. Anderson, J. A. Reusch, D. Liu, G. Fiksel, S. Polosatkin, and V. Belykh, Rev. Sci. Instrum. **83**, 10D302 (2012).
[39]S. Eilerman, "Ion runaway during magnetic reconnection in the reversed-field pinch," Ph.D. dissertation, University of Wisconsin–Madison (2014).
[40]R. W. Harvey and M. G. McCoy, in *Proceedings of IAEA/TCM on Advances in Simulation and Modeling of Thermonuclear Plasmas*, Montreal (1992), p. 489–526.
[41]R. J. Goldston, D. C. McCune, H. H. Towner, S. L. Davis, R. J. Hawryluk, and G. L. Schmidt, J. Comput. Phys. **43**, 61 (1981).
[42]J. A. Reusch, J. K. Anderson, and Y. A. Tsidulko, Nucl. Fusion **54**(10), 104007 (2014).